Aspects of the band structure of $CuGaS_2$ and $CuGaSe_2$

B. Tell and P. M. Bridenbaugh
Bell Laboratories, Holmdel, New Jersey 07733
(Received 18 June 1975)

The spin-orbit splitting has been determined in the sulfur-rich section of the system $CuGaS_{2-2x}Se_{2x}$, which demonstrates that the spin-orbit splitting is negative in $CuGaS_2$. A model which provides adjustable coupling and separation between the p- and d-like valence band can account for the main features of the band structure of $CuGaS_2$ and $CuGaSe_2$.

I. INTRODUCTION

There has been much recent interest in the band structure of I-III-VI_2 compounds.[1-3] These compounds are characterized by a large reduction in the energy band gap and in spin-orbit splitting as compared to their binary analogs. For example, the energy gap of $CuGaS_2$ is ~2.5 eV, while its binary analog ZnS has an energy gap of ~3.9 eV.[2] The spin-orbit splitting of ZnS is +70 meV, while $CuGaS_2$ is ~17 meV. In addition, the sign of the spin-orbit splitting in $CuGaS_2$ is probably negative but has not been definitely established.[4] For $CuGaSe_2$, the band gap is reduced by ~1 eV and the spin-orbit splitting is reduced from ~0.45 to 0.23 with respect to its analog ZnSe.[2] These effects have been attributed to the proximity and consequent hybridization of the noble-metal d bands with the p bands on the other atoms. The hybridized nature of the p and d bands has been observed directly in x-ray photoemission[5-7] and electroreflectance studies.[8]

In this paper, we present a model for the band structure of the I-III-VI_2 compounds. This model contains two parameters, the energy separation between the noninteracting p and d bands and the interaction strength between these bands. With a judicious selection of these parameters, the main features of the band structure can be explained. In addition, we present experimental results which show that the spin-orbit splitting is definitely negative in $CuGaS_2$ and varies smoothly in the system $CuGaS_{2-2x}Se_{2x}$. That is, as a function of alloy composition in the $CuGaS_{2-2x}Se_{2x}$ system, the spin-orbit splitting varies from -0.017 eV ($x=0$) to ~+0.23 eV ($x=1$).

II. EXPERIMENTAL PROCEDURE

The crystals were iodine transported, grown by the method of pulling the ampoule through a vertical thermal gradient.[9] The maximum temperature was ~900 °C, slightly less than previously used for the growth of $CuGaS_2$ (950 °C). Much selection was required in order to find a crystal or a section of a crystal with an adequate wavelength derivative reflectivity (WDR) signal.

All data were taken with the samples immersed in liquid nitrogen. The wavelength modulator consisted of a 3-mm-thick quartz plate placed near the exit slit of a $\frac{3}{4}$-m Spex spectrometer. The plate vibrated at 20-Hz and produced a ~3-Å wavelength modulation. The spectrometer slit width was also chosen to be ~3 Å. The 20-Hz modulated signal was amplified with a phase sensitive detector, and provision was made for normalizing the signal, i.e., dividing by the incident dc intensity. In the small-wavelength regions employed, dividing generally did not make any significant difference.

The WDR data were appreciably sharper and stronger for a typical $CuGaS_2$ crystal than for a typical $CuGaSe_2$ crystal. This was fortunate since the S-rich region is the one of present interest. The alloy compositions were determined by assuming a linear variation of the energy of the A exciton. Moderate agreement was obtained with similar determinations assuming a linear variation of the lattice constants, which were obtained from powder patterns. However, the lattice-constant method resulted in considerable scatter due to a probable difference in surface-to-bulk compositions.

III. BACKGROUND AND EXPERIMENTAL RESULTS

The chalcopyrite band structure for the uppermost valence-band to conduction-band transition is shown in Fig. 1.[10] Under the combined influence of crystal-field and spin-orbit splittings, the original threefold degeneracy of the p-like valence band is completely lifted. The valence- to conduction-band transitions are conventionally labeled A, B, and C in terms of increasing energy. The usual valence-band ordering (Γ_7, Γ_6, Γ_7) and the polarization-selection rules are also indicated. Shay *et al.*[10] obtained good agreement with experimental results for the II-IV-V_2 compounds by assuming the band-gap and spin-orbit splitting

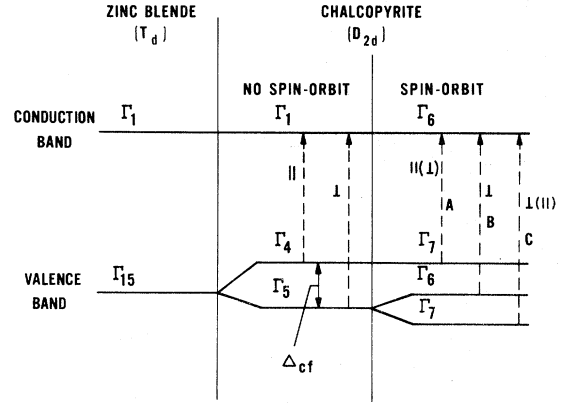

FIG. 1. Energy band structure near the center of the Brillouin zone showing the transition from zinc blende to chalcopyrite. The selection rules, with respect to the optic axis, are indicated. The symmetry designations have been previously used (Refs. 1, 2).

were equal to that of the binary analogue (i.e., InP is the binary analogue of $CdSnP_2$ and $In_{0.5}Ga_{0.5}As$ is the binary analogue of $CdGeAs_2$). Furthermore, the crystal-field splitting Δ_{cf} could be estimated simply from the formula $\Delta_{cf} = -b(1 - c/2a)$. Here, c and a are the lattice constants parallel and perpendicular to the z or optic axis, respectivly, and b is a deformation potential with typical magnitude of ~ 1 eV. The quantity $1 - c/2a$ is the measure of the lattice compression, since $c/2a$ is generally less than unity.

For the I-III-VI_2 compounds, the simple binary analog produces poor agreement with experimental results. The band gap in $CuGaS_2$ and $CuGaSe_2$ is more than 1 eV less than the binary analog, the spin-orbit splitting is reduced from + 70 to − 17 meV in the sulfides and from ~ + 430 to + 230 meV in the selenides. We will show that these discrepancies can be accounted for with the model presented below. There is also a discrepancy in the crystal-field splitting, which is invariably larger than estimated from the simple compression formula. This latter discrepancy will not be treated in the present model.

Referring again to Fig. 1, the A-B splitting is related to the crystal-field splitting and the B-C splitting is related to the spin-orbit splitting. These relations are given by the quasicubic model and have been described in detail in previous publications.[10,11] $CuGaS_2$ and $CuGaSe_2$ have approximately the same noncubic distortion, i.e., $1 - c/2a$, so that the A-B splitting should have similar magnitude, whereas the B-C splittings, related to spin orbit, should be greatly different. We will show below that ordering of the valence bands in $CuGaSe_2$ is that given by Fig. 1, while in $CuGaS_2$ the Γ_6 valence band is deepest in energy. This inversion is referred to as negative spin-orbit splitting.

The 77 °K WDR spectrum for $CuGaSe_2$ is shown in Fig. 2. The energies for the A, B, and C transitions are 1.729, 1.813, and 2.016 eV, respectively, which yields the crystal-field splitting $\Delta_{cf} = -112$ meV and the spin-orbit splitting $\Delta_{so} = +231$ meV.[11] These values are in reasonable agreement with previous room-temperature electrolyte electroreflectance results.[1,2] The WDR for $CuGaS_2$, obtained from Ref. 4, is, for convenience, reproduced in Fig. 3. The energies of the A, B, and C transitions are 2.502, 2.627, and 2.638 eV, respectively, which yields $\Delta_{cf} = -130$ meV and $\Delta_{so} \approx \pm 17$ meV.[4,11] The ordering of the B and C transitions is difficult to determine from polarization studies alone, so that the ordering is partly determined from knowledge of the expected splittings. The polarization-intensity ratios for the Γ_7 valence bands to Γ_6 conduction-band transitions are given by

$$I_{\parallel}/I_{\perp} = (2 - 3\Delta E/\Delta_{so})^2 , \qquad (1)$$

where ΔE is the separation from the totally perpendicularly polarized $\Gamma_6 \rightarrow \Gamma_6$ transition.[11] This difficulty for $CuGaSe_2$ is mainly due to crystal misorientation, since the natural faces from which WDR reflectivity can be obtained have (112) orientation. This orientation allows total perpendicular polarization, but is only nominal for parallel polarization.[10] That is, parallel polarization is $\frac{2}{3} I_{\parallel} + \frac{1}{3} I_{\perp}$, so that a totally perpendicular polarized transition exhibits only a 1:3 intensity variation

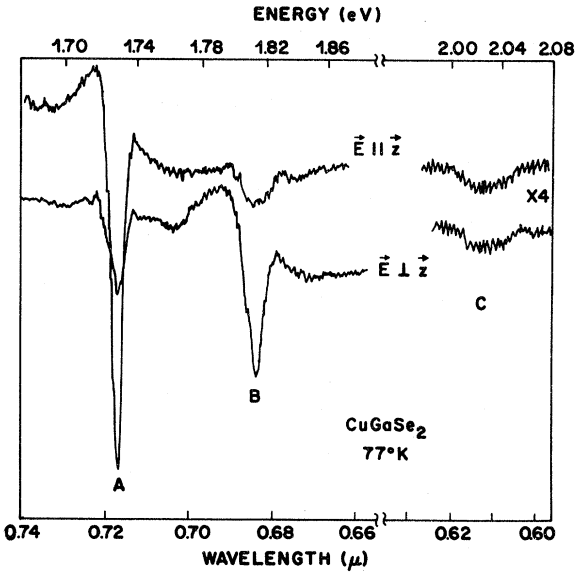

FIG. 2. 77 °K WDR spectrum for a (112) face of $CuGaSe_2$ for light polarized parallel and perpendicular to the optic axis.

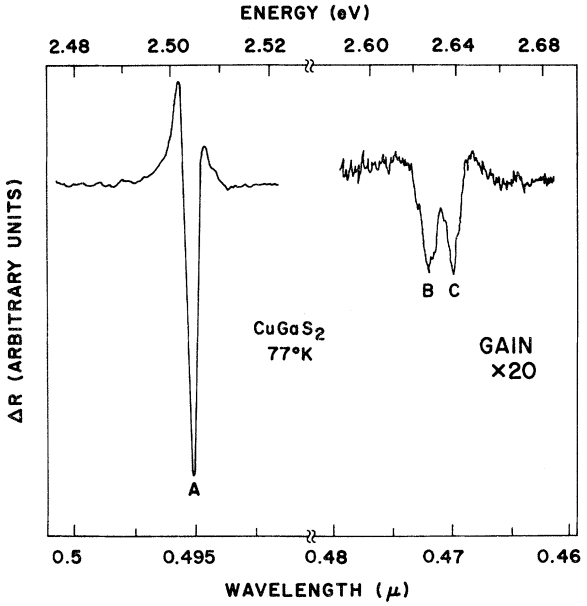

FIG. 3. WDR spectrum for $CuGaS_2$ reproduced from Ref. 4. The A transition is shown for $\vec{E} \parallel \vec{Z}$ and the B, C for $\vec{E} \perp \vec{Z}$.

due to the crystal misorientation. The calculated polarization-intensity ratios with respect to the z axis for the A, B, and C excitons [from Eq. (1), including the misorientation effects] are 7:1, 1:3, and 2:3. The observed ratios are approximately 5:1, 1:4, and 1:1. The trend is correct and confirms the Γ_7, Γ_6, Γ_7 valence-band ordering for $CuGaSe_2$. For $CuGaS_2$, due to the small spin-orbit splitting, the lower energy $\Gamma_7 \rightarrow \Gamma_6$ transition is nearly totally parallel polarized, while for the higher energy $\Gamma_7 \rightarrow \Gamma_6$ is nearly totally perpendicularly polarized. Consequently, the ordering of the B and C excitons cannot be determined from polarization measurements.

The energy-band splittings of the $CuGaS_2$-$CuGaSe_2$ system are plotted in Fig. 4. A linear interpolation is drawn between the three transitions. Since the sign of the B-C splitting is not known *a priori* in $CuGaS_2$, two lines are drawn for the two higher-energy transition. The solid lines are the interpolation for a negative spin-orbit splitting and the dashed lines, for a positive spin-orbit splitting. For a negative spin-orbit splitting, the B-C separation should go to zero for a ~ 5 % Se content, while for a positive spin-orbit splitting, the separation should continuously increase.

In Figs. 5 and 6, the WDR spectra for two alloys are shown. In Fig. 5, the B-C splitting is not resolved, and the two solid lines at the B-C transition indicate the expected splitting if the spin-orbit splitting were positive. This expected splitting is greater than the B-C line width, and in itself is strong evidence that the spin-orbit splitting is negative. In Fig. 6, the splitting is resolved, even though the line widths are considerably broader than the line widths for the spectra presented in Fig. 5. These, and several other experimental points are plotted in Fig. 4. There appears little doubt that the solid lines represent the experimental situation. That is, the spin-orbit splitting is indeed negative in $CuGaS_2$.

IV. BAND-STRUCTURE MODEL

A simple model which explained the salient features of the band structure of I-III-VI_2 compounds could be of interest. In the first approximation, one simplifies to cubic crystals and considers only the center of the Brillouin zone. The original threefold degenerate p level (Γ_{15}) is split by spin-

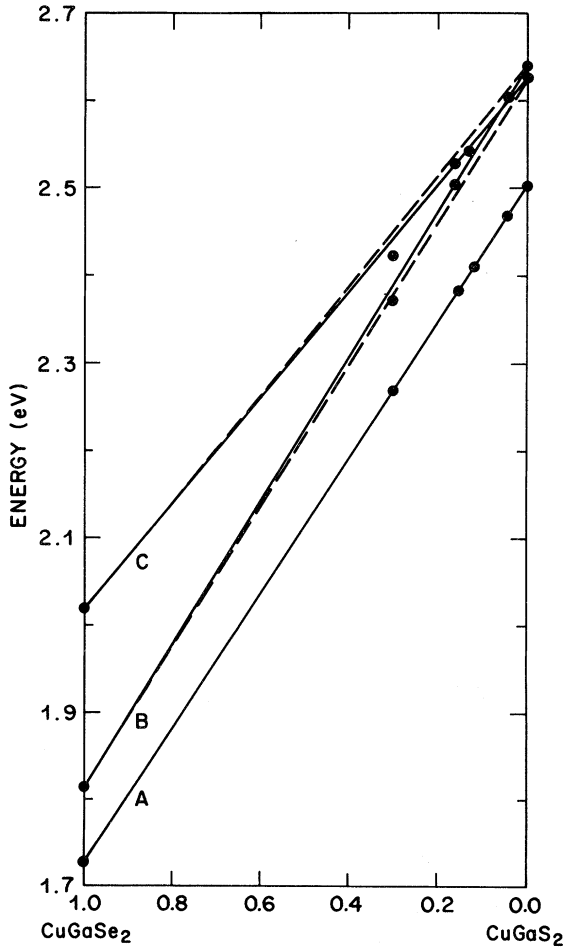

FIG. 4. Linear interpolation of the 77 °K A, B, and C excitons for the end members in the system $CuGaS_{2-2x}Se_{2x}$. The solid lines represent the interpolation for a negative spin-orbit splitting and the dashed lines for a positive spin-orbit splitting in $CuGaS_2$. The closed circles are the experimental points.

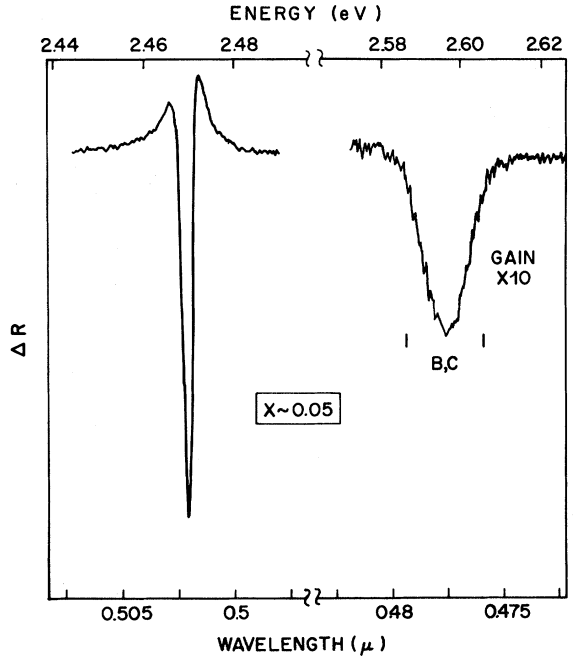

FIG. 5. WDR spectrum for $CuGaS_{2(0.95)}Se_{2(0.05)}$. The solid lines at the outside of the B, C transition indicates the expected splitting for the $B-C$ excitons if the spin-orbit splitting was positive in $CuGaS_2$.

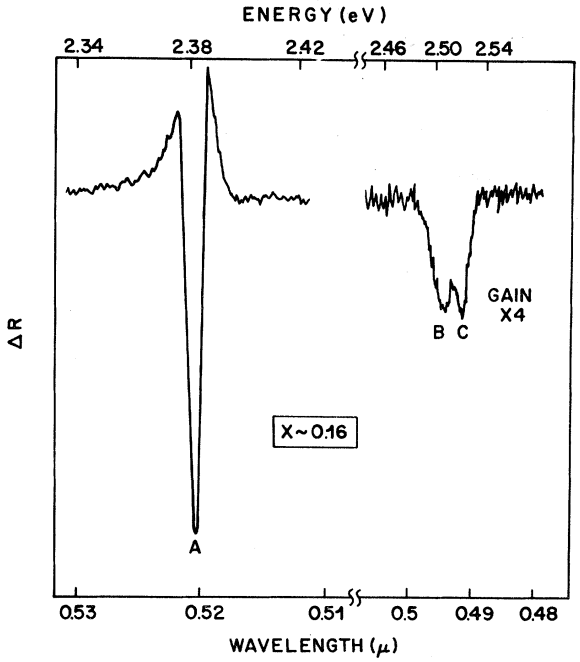

FIG. 6. WDR spectrum for $CuGaS_{2(0.84)}Se_{2(0.16)}$ showing the reappearance of the splitting of the B, C excitons in spite of the increase in line widths from Figs. 4 and 5.

orbit interaction into a singlet (Γ_7) and a doublet (Γ_8) with the doublet lying above the singlet, as shown in the right-hand side of Fig. 7. The five-fold degenerate d level splits into a doublet and a triplet, the triplet having the same symmetry (Γ_{15}) as the p level. Under the influence of the tetrahedral field, the doublet is presumed to lie at higher energy than the triplet. In any case, the doublet has the wrong symmetry (Γ_{12}) to interact with the triplets, and we assume its influence can be neglected. Under the influence of the spin-orbit interaction, the d triplet is inverted (Fig. 7) as originally deduced by Cardona[12] and mathematically derived by Shindo *et al.*[13] This inversion is referred to as negative spin-orbit splitting.

There are two parameters in this model, the energy separation E between the p and d levels and the interaction M between these levels. The p and d triplets have the same symmetry, and it is reasonable to expect an interaction and overlap of their wave functions since the simplest tight-binding approximation, the p-like valence band lies on the S atom, while the d-like valence band lies on the Cu atom, the Cu and S atoms being nearest neighbors. The basis of the model is that two levels of the same symmetry will mix and repel each other, with magnitude depending on the energy separation and strength of the interaction potential. This mixing is responsible for both the reduction in the energy band gap and for the reduced or negative spin-orbit splittings.

Let the wave functions for the noninteracting p and d levels be a set of orthonormalized states $\phi_p(\Gamma_8)$, $\phi_p(\Gamma_7)$, $\phi_d(\Gamma_8)$, and $\phi_d(\Gamma_7)$. In the presence of an interaction, the wave functions are

$$\begin{aligned}
\psi_1(\Gamma_8) &= a_1\phi_p(\Gamma_8) + b_1\phi_d(\Gamma_8)\ , \\
\psi_2(\Gamma_8) &= a_2\phi_p(\Gamma_8) + b_2\phi_d(\Gamma_8)\ , \\
\psi_1(\Gamma_7) &= a_3\phi_p(\Gamma_7) + b_3\phi_d(\Gamma_7)\ , \\
\psi_2(\Gamma_7) &= a_4\phi_p(\Gamma_7) + b_4\phi_d(\Gamma_7)\ .
\end{aligned} \tag{2}$$

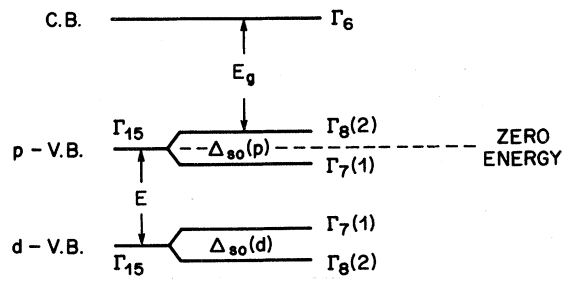

FIG. 7. Sketch of the band extrema near $\vec{k}=(0,0,0)$ showing the p and d valence bands as split by the spin-orbit interaction. The energy gap E_g and the level degeneracies are also indicated. The degeneracies are not presently relevant, since Γ_8 doublets are not split in the context of the given model. The energy E is measured from the center of the p levels to the center of the d levels and is positive as illustrated.

The noninteracting p and d levels are diagonal with energies given by $+\frac{1}{2}\Delta_{so}(p)$, $-\frac{1}{2}\Delta_{so}(p)$, $E+\frac{1}{2}|\Delta_{so}(d)|$, and $E-\frac{1}{2}|\Delta_{so}(d)|$, respectively. $\Delta_{so}(p)$ is characteristic of the spin-orbit splitting of the II-VI sulfides and is taken as +70 meV, while $\Delta_{so}(d)$ is characteristic of Cu spin-orbit splitting and is taken as −150 meV.[14] The interactions are defined by

$$\langle \phi_p(\Gamma_8)|V_{pd}|\phi_d(\Gamma_8)\rangle = \langle\phi_p(\Gamma_7)|V_{pd}|\phi_d(\Gamma_7)\rangle = M\ , \tag{3}$$

and

$$\langle\phi_p(\Gamma_7)|V_{pd}|\phi_d(\Gamma_8)\rangle = \langle\phi_p(\Gamma_8)|V_{pd}|\phi_d(\Gamma_7)\rangle = 0\ , \tag{4}$$

where V_{pd} is the interaction potential whose matrix elements are either zero or M. The Hamiltonian matrix then takes the following form:

$$\begin{bmatrix} \frac{1}{2}\Delta_{so}(p) & M & 0 & 0 \\ M & E-\frac{1}{2}|\Delta_{so}(d)| & 0 & 0 \\ 0 & 0 & -\frac{1}{2}\Delta_{so}(p) & M \\ 0 & 0 & M & E+\frac{1}{2}|\Delta_{so}(d)| \end{bmatrix} . \tag{5}$$

Using E and M as parameters, the matrix is diagonalized to yield both the eigenvalues and the square of the eigenvectors (hybridization). The hybridization of a particular level is given by, for example,

$$\langle\psi_1|\psi_1\rangle = a_1^2 + b_1^2 = 1\ , \tag{6}$$

where a_1^2 is the percentage of p-like character in a given energy band, and $b_1^2 = 1 - a_1^2$ is the percentage of d-like character for the same band.

The results of the calculation for $CuGaS_2$ are given in Fig. 8. (This calculation applies equally well to $CuInS_2$.) The energy-level shifts are plotted with respect to the energy separation E between the noninteracting p- and d-like levels for various interaction strengths M. The straight lines are the noninteracting levels (i.e., $M = 0$). It is seen from the figure that for E large and negative (i.e., the d bands above the p bands), the upper levels asymptotically approach the pure d-like levels and have a negative spin-orbit splitting characteristic of the copper d levels. Similarly, for large positive E, the levels have predominantly p-like character and a positive spin-orbit splitting characteristic of the sulfur p levels.

The observed energy-gap shift between $CuGaS_2$ and the assumed pure p-like levels of its binary analogue ZnS is ~1.4 eV. (Experience leads us to estimate that between 1.0–1.2 eV of this shift is due to the presence of the d levels. However, the exact amount is not known and is not presently significant.) An energy-gap shift of 1.0 to 1.2 eV with a negative spin-orbit splitting of ~17 meV is given by an interaction parameter $M \sim 1.0$ eV, as shown by the boxed region in Fig. 8. In this region, the hybridization is approximately 50 %, being slightly more d-like than p-like. For this given noninteracting separation E (between 0 and −0.5 eV), a set of higher energy bands should exist roughly 2 eV from the upper valence bands. Such bands are indeed seen in the electroreflectance spectra for both $CuGaS_2$ and $CuInS_2$.[15]

In Fig. 9, the results of a similar calculation for $CuGaSe_2$ are shown (applying equally well to $CuInSe_2$), the only differences being the larger spin-orbit splitting characteristic of II-VI selenides (~0.43 eV) and the somewhat smaller downshift in the energy gap of $CuGaSe_2$ with respect to the assumed pure p-like levels of ZnSe. The shift is about 1 eV, of which we assume ~0.8 eV is due to the presence of the Cu d levels. We find that an interaction parameter of ~1 eV produces a shift of ~0.8 eV for the top valence band and

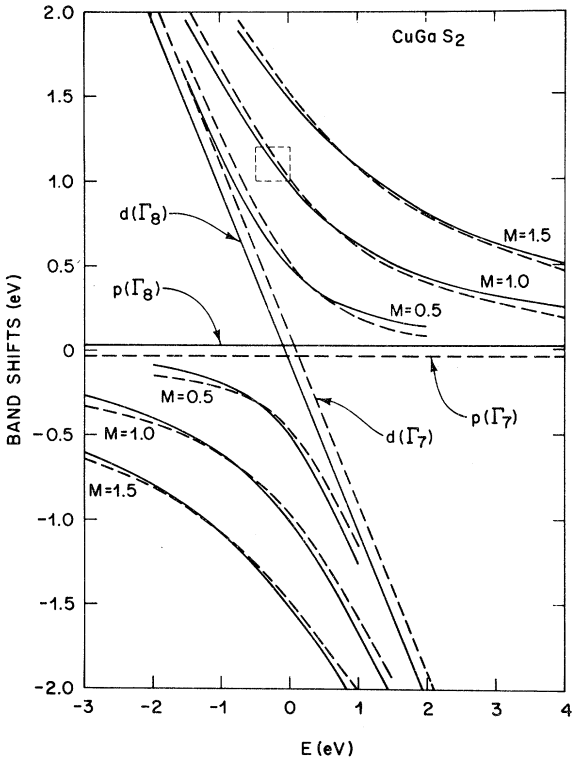

FIG. 8. Energy position and symmetry for the upper and lower valence bands for continuous variation of E and stepwise variation of M for $CuGaS_2$. The straight horizontal lines represent the noninteracting p levels, and the straight diagonal lines represent the noninteracting d levels. In all cases, the solid curves are for Γ_8 symmetry and the dashed curves for Γ_7.

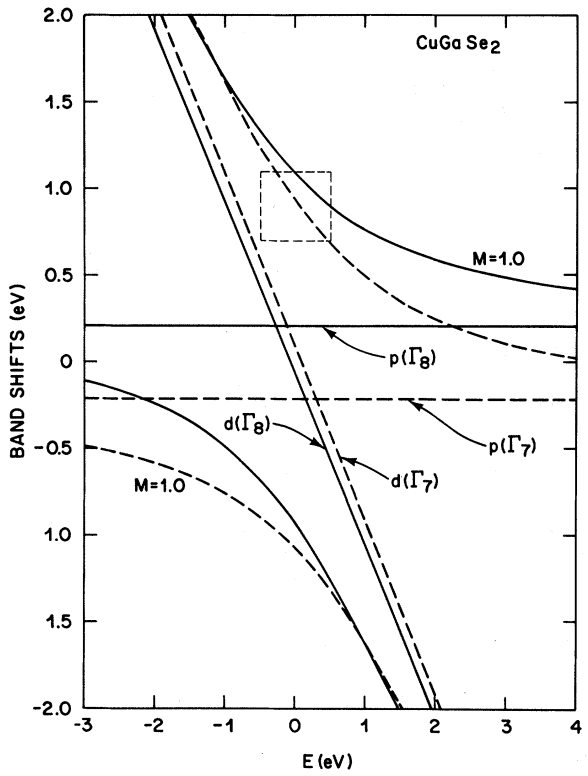

FIG. 9. Same as for Fig. 8, except that the p-level spin-orbit parameter was taken to be characteristic of the selenides.

reduces the spin-orbit splitting to ~0.2 eV. Again, the model predicts a higher set of valence bands about 2 eV from the top valence band. Such bands have been observed in the electroreflectance spectra of $CuInSe_2$ and ascribed to Cu d bands.[8] Similar bands were not observed in $CuGaSe_2$ in electroreflectance measurements, presumably due to the poorer quality of the available crystals.

We find it remarkable that this simple model can fit the observed energy band structure of the I-III-VI_2 compounds. It clearly shows how the spin-orbit splitting varies from small and negative in both $CuGaS_2$ and $CuInS_2$ to large (however greatly reduced from ZnSe and CdSe) and positive in $CuGaSe_2$ and $CuInSe_2$. It can also explain the downshifts in the energy gaps of the strongly hybridized Cu I-III-VI_2 compounds with respect to the II-VI compounds. In addition, further structure is seen in electroreflectance spectra which occurs in the energy region consistent with this model.

The model could also be extended to include the Ag I-III-VI_2 compounds. For the Ag compounds, the energy-gap shift is less, but the reduction in spin-orbit splitting is about the same as the Cu compounds. However, the hybridization calculated for Ag compounds is smaller than for the Cu compounds, as originally deduced by Shay *et al.*[1,2] and confirmed by recent x-ray photoemission studies.[5-7] These results can be explained by the larger negative spin-orbit splitting associated with Ag atoms (~0.33 eV),[14] so that a comparable reduction in spin-orbit splitting can occur even for reduced hybridization and energy-gap shift.

In conclusion, from studying the spin-orbit splitting in S-rich alloys, we have shown that the spin-orbit splitting is negative in $CuGaS_2$. In addition, we have shown that the band structure of ternary sulfides and selenides can be fit with a hybridized p-d-band model with similar parameters.

[1]For reviews, see J. L. Shay and B. Tell, J. Surf. Sci. 37, 748 (1973); J. L. Shay and J. H. Wernick, *Ternary Chalcopyrite Semiconductors: Growth, Electronic Properties and Applications* (Pergamon, New York, 1975).

[2]J. L. Shay, B. Tell, H. M. Kasper, and L. M. Schiavone, Phys. Rev. B 5, 5003 (1972).

[3]J. L. Regolini, S. Lewonczuk, J. Ringneissen, S. Nikitine, and C. Schwab, Phys. Status Solidi 55, 193 (1973).

[4]B. Tell, J. L. Shay, H. M. Kasper, and R. L. Barns, Phys. Rev. B 10, 1748 (1974).

[5]M. J. Luciano and C. J. Vesely, Appl. Phys. Lett. 23, 60 (1973); *ibid.* 23, 453 (1973).

[6]S. Kono and M. Okusawa, J. Phys. Soc. Jpn. 37, 1301 (1974).

[7]W. Braun, A. Goldmann, and M. Cardona, Phys. Rev. B 10, 5069 (1974).

[8]J. L. Shay and H. M. Kasper, Phys. Rev. Lett. 29, 1162 (1972).

[9]J. L. Shay, P. M. Bridenbaugh, and H. M. Kasper, J. Appl. Phys. 45, 4491 (1974); P. M. Bridenbaugh and B. Tell, Mat. Res. Bull. (to be published).

[10]J. L. Shay, E. Buehler, and J. H. Wernick, Phys. Rev. B 2, 4104 (1970); J. L. Shay and E. Buehler, *ibid.* 3, 2598 (1971).

[11]J. E. Rowe and J. L. Shay, Phys. Rev. B 3, 451 (1971).

[12]M. Cardona, Phys. Rev. 129, 69 (1963).

[13]K. Shindo, A. Morita, and H. Kaminura, J. Phys. Soc. Jpn. 20, 2054 (1965).

[14]M. Cardona, *Modulation Spectroscopy* (Academic, New York, 1969).

[15]B. Tell, J. L. Shay, and H. M. Kasper, Phys. Rev. B 4, 2463 (1971).